Time-dependent computations of turbulent bluff-body diffusion flames close to extinction

P. Koutmos, C. Mavridis and D. Papailiou
Department of Mechanical Engineering, University of Patras, Greece

Received September 1997
Revised May 1998
Accepted September 1998

Keywords *Bluff-body, Combustion, Navier-Stokes equation*

Abstract *A two dimensional time-dependent Navier Stokes formulation that encompasses aspects from both the LES formalism and the conventional k-ε approaches was employed to calculate a range of reacting bluff-body flows exhibiting high or low level large scale structure activity. Extensive regions of local flame extinction found in these bluff-body flame configurations were treated with a partial equilibrium/two-scalar exponential PDF combustion submodel combined with a local extinction criterion based on a comparison of the turbulent Damkohler number against the ratio of the scalar scale to the reaction zone thickness. A dual-mode description, burning/non-burning, of combustion provided the local gas state. Comparisons between calculations and measurements indicated the ability of the method to capture all the experimentally observed variations in the momentum and reactive scalar mixing fields over a range of operating conditions from the lean to the rich blow-out limit.*

Nomenclature

C_μ = turbulent viscosity coefficient
D = square cylinder diameter
d = fuel jet diameter in axisymmetric bluff-body
f = mixture fraction
f^* = normalized mixture fraction
$f_{L,R}$ = Lean/rich mixture fraction flammability limits
FAR = Fuel-air ratio
FAVR = Fuel-air velocity ratio
J = Jacobian of transformation
k = turbulence kinetic energy
k_{tot} = total fluctuating energy (periodic + turbulent)
k_f = forward reaction rate
k_e = equilibrium constant
L_t, l = turbulence length scales
MR = Momentum ratio
u, v = axial and transverse velocities
U_o, u_o = approach air flow velocity
P, PDF = Probability density function
$\dot{r}_{co_2}$ = reaction rate of CO_2
Re_t = turbulent Reynolds number
R_u = universal gas constant
S_{ij} = strain rate tensor
St = Strouhal number
T = temperature
t_o = characteristic time (=D/u_o)
x_i = coordinate directions (i = 1, 2)
Y_i = mass concentration
Y^*_{C02} = normalized concentration of CO_2
Y^E = undisturbed burning state vector
Y^I = inert mixing state vector

Greek symbols

δ_{ij} = Kronecker delta ($\delta_{ij} = O$ for $i \neq j$, $\delta_{ij} = 1$ for $i = j$)
Δ, Δx, Δy = characteristic mesh sizes
ε = dissipation rate of the scalar fluctuations
ϕ = conserved scalar
ν_t = eddy-viscosity coefficient
ρ = density
Σ_f = Gibson scale
σ_t = turbulent Prandtl number
τ_t = time-scales of turbulence
τ_{ch} = time scale of chemical reaction
τ_k = Kolmogorov time scale

Operators

<...> = ensemple or phase-averaged (resolved) quantity
<...> = time-averaged
$(...)^{/}$ = turbulent (subgrid) fluctuation
$(...)^{//}$ = large scale (resolved) fluctuation

(*Continued*)

International Journal of Numerical Methods for Heat & Fluid Flow, Vol. 9 No. 1, 1999, pp. 39-59,

$\langle \tilde{...} \rangle$	=	Favre (density)-weighted value
$P(f, x_i)$	=	probability density function

Subscripts

A, a	=	air
E	=	explicitly (cumulatively-statistically) calculated
F, f	=	fuel
i	=	i = 1, 2 Cartesian coordinates
i, j	=	tensor notation
L	=	Lean
R	=	Rich
t	=	turbulent flow
s	=	stoichiometric

Superscripts

*	=	normalized value
+	=	wall coordinates

1. Introduction

The recirculation of high temperature combustion products is frequently employed in combustion systems to improve fuel-air mixing rates and reduce pollutant emissions (Mellor, 1990). Bluff-body systems provide such a typical recirculation whereby the aerodynamic interaction between the injected fuel (in jet or other form) and the vortex is conducive to flame stabilization and control over wide ranges of air velocities, fuel injection rates and turbulent time and length scales (Masri *et al.,* 1994; Roquemore *et al.,* 1983; Schefer *et al.,* 1987). Apart from its practical relevance this configuration provides a useful research tool for experimental and numerical studies of turbulent reacting flows (Libby and Williams, 1993).

In recent years the advent of efficient Reynolds (or Phase)-averaged Navier-Stokes solvers coupled with the need to reduce combustor development costs has established CFD methods as a valuable tool for turbulent combustion studies (Bilger, 1988; Peters, 1988; Pope, 1990). Traditionally, jet flames have provided a suitable test bed for developing combustion models, since their aerodynamic fields are easier to compute. The simulation of practical combustors, however, necessitates the formulation, testing and appraisal of combustion models in recirculating flames that possess some characteristics relevant to the practical device (Correa and Gulati, 1992; Correa *et al.,* 1994), e.g. increased dissipation and strain rates, strong turbulence/chemistry coupling or large scale vortex interactions with the flame zone.

Recent experimental works on bluff-body flames (Masri *et al.,* 1994, 1988; Schefer *et al.,* 1987) have reported non-intrusive space and time-resolved measurements, providing valuable insight into the local flame structure, extinction characteristics and transient flame behaviour and have identified a range of parameters that characterise non-premixed flames (Bilger, 1988). These have greatly aided in the effort to extend available models such as the partial equilibrium/assumed shape PDF of Correa and Gulati (1992), the Lagrangian approach of Obounou *et al.* (1994), the PDF transport method of Correa *et al.* (1994) and the eddy dissipation concept of Gran *et al.* (1994) to treat bluff-body stabilised flames.

Although the treatment of finite-rate chemistry effects and their interaction with turbulence is definitely a significant driver of current technology, a number of experimental and computational works (Kaplan *et al.,* 1994; Koutmos *et al.,* 1996; Ohiwa *et al.,* 1994; Roquemore *et al.,* 1983) has also strongly emphasised the influence of large scale vortex structures and flow

unsteadiness on entrainment, heat release and stability of both jet and bluff-body flames. This is particularly relevant for flames operated in the air-flow dominated regime (Koutmos *et al.,* 1996; Roquemore *et al.,* 1983; Schefer *et al.,* 1987) as most frequently encountered in practical combustors under lean overall conditions. Furthermore, the active role played by large scale vortex structures is clearly enhanced as bluff-body flames approach extinction (Kaplan *et al.,* 1994; Ohiwa *et al.,* 1994; Roquemore *et al.,* 1983; Schefer *et al.,* 1987) leading to unsteady phenomena which affect both micro- and macro-scales of the reacting flow (Neveu *et al.,* 1996). These effects merit evaluation through inclusion in computations capable of representing unsteady large scale motions. By adequately resolving these dynamic features of the reacting flow a better exploitation of the combustion submodel may be achieved along with a more appropriate inclusion of finite-rate kinetic effects.

The present work therefore attempts to tackle the above issues and develop a tool for studying bluff-body flames close to extinction with or without the influence of large scale structures and flow unsteadiness. A two-dimensional time-dependent phase-averaged Navier-Stokes procedure which was successfully employed to predict unsteady separated non-reacting flows (Koutmos and Mavridis, 1997) is here extended to calculate the scalar mixing and reaction in bluff-body flames. Flows which exhibit periodic, quasi-periodic or flapping motions as frequently encountered in flame stabilisation are hereby analysed consistently with a global approach. The method is combined with a partial equilibrium/two-scalar exponential PDF model to treat turbulence/chemistry interactions. Statistical independence of the PDF variables is avoided, in the light of recent experimental work (Cheng and Pitz, 1994), and the required PDF moments are evaluated through simplified expressions reduced from their full transport equations.

Finite-rate kinetic effects such as partial extinction and reignition, which are important for evaluating burner stability, are handled by comparing the local mixing time scale with the chemical time scale supplied by the reactive scalar in the two-scalar PDF formulation. Under extinction conditions the chemical source terms of the reactive scalar are set to zero and the quenched region is treated as an inert mixing region.

The model is validated against non-intrusive measurements in two bluff-body flames exhibiting significant degrees of local extinction. The first is a methane-jet-fuelled axisymmetric bluff-body configuration operated in the jet dominated regime, i.e. the fuel jet penetrates through the primary recirculation, and has been studied by Correa *et al.* (1994). The second is a propane diffusion flame formed by planar fuel jet injection into the vortex formation region of a slender two-dimensional square cylinder operated in the air-flow dominated regime, i.e. with no fuel jet penetration through the main vortex, and has been studied by Bakrozis *et al.* (1994) and Koutmos *et al.* (1996). While in this configuration interactions between large scale vortex structures and the flame zone are significant, the axisymmetric case does not manifest such unsteady phenomena. The selected cases therefore test the model's ability in a diversity of complex turbulent flames and allow a direct comparison with other modelling approaches.

2. Details of bluff-body configurations studied

Figures 1a and 1b depict the burner geometries studied in the present work. The axisymmetric bluff-body geometry in Figure 1a is the same one studied in Correa *et al.* (1994). The flameholder, contained within a square cross-section wind tunnel of $15.2 \times 15.2 cm^2$, has an outer diameter of 38mm with a concentric fuel jet of 3.18mm diameter. Raman data on mixture fraction, temperature and major species have been presented in Correa *et al.* (1994) for this geometry. Since the tunnel dimensions are much greater ($\times$ 4) than the bluff-body diameter the computational domain was here represented by an axisymmetric mesh with the outer radial dimension chosen to preserve the cross-sectional area of the square duct. The fuel jet/annulus air flow velocity ratio in that study was (62.5/18) m/s with inlet conditions of 1atm and 300K. With this velocity ratio the burner operates in the jet-dominated regime with recirculation effects confined to the base of the jet, on the bluff-body face, where

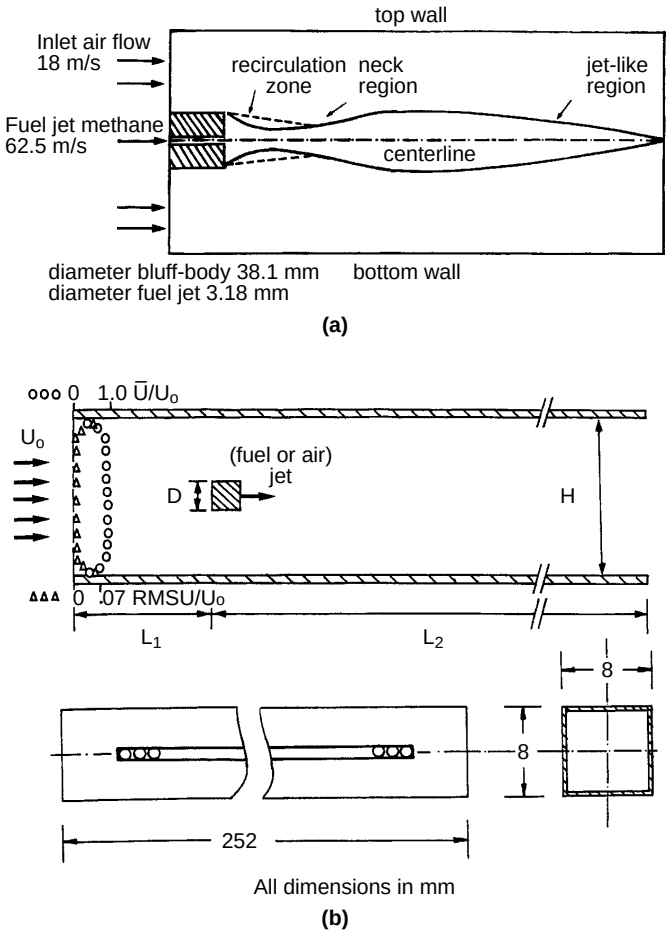

Figure 1.
Flow configuration and geometry of bluff-body combustors, (a) axisymmetric burner; (b) slender 2D cylinder

stabilization is desired. Significant localized extinction has been measured downstream of the bluff-body face at x/d≈20 with reignition further downstream at x/d≈30.

The wind tunnel and a sketch of the square cross-section hollow cylinder burner used in the second computational investigation are shown in Figure 1b. The 8mm diameter burner was inserted into a rectangular cross-section duct of $42 \times 252 mm^2$ producing an area blockage of 0.19. Propane was fed through the cylinder ends and injected into the cylinder wake through 125 holes, 1mm in diameter and spaced at 0.2mm apart on the symmetry plane (Figure 1b). In the simulations the injection system was modeled as a spanwise slot of 1mm height maintaining the correct momentum efflux per unit span and allowing for increased fuel inlet turbulence levels. This set up has been measured extensively by Bakrozis *et al.* (1994), for a range of Reynolds numbers and fuel to approach air velocity ratios. Detailed profiles of the mean and turbulent axial and cross-stream velocities and temperatures with corresponding statistics have been obtained throughout the near and far wake regions. Laser velocimetry and high temperature Pt-Pt/10%Rh uncoated butt-welded thermocouples were used to obtain these measurements.

For comparisons with the present model an ultra-lean (overall equivalence ratio of 0.01655) short blue-coloured flame in the air-flow dominated regime (no jet penetration through the primary vortex) with a fuel-air velocity ratio (FAVR) of 0.189 (Reynolds number based on air approach velocity 8,520) was chosen in the present discussion. This flame is also operated close to its global extinction limit, which is achieved at a FAVR of 0.11. The important controlling parameter is the fuel/primary air momentum ratio ($MR=(\rho_F/\rho_A)*FAVR^2$) and this has a value of 0.0208 for this flame.

3. Numerical method

3.1 Aerodynamic model

The isothermal and reacting wakes were calculated with the 2D time-dependent N-S equations governing the temporal and spatial variation of the velocities and pressures, e.g. $u = \langle u \rangle + u'$ with $\langle u \rangle = \bar{u} + u''$ where u and $\langle u \rangle$ are the instantaneous and phase-averaged (or resolved) velocities, $\bar{u}$ and u'', the time-mean and large-scale (resolved) fluctuating components and u' the stochastic (subgrid) turbulent fluctuation. The model description given below closely follows the formulations adopted in Koutmos and Mavridis (1997). For the reacting flows density-weighted values are used i.e. $\langle \tilde{f} \rangle = \overline{\rho \langle f \rangle}/\bar{\rho}$. The equation set may be written as follows:

$$\frac{\partial \bar{\rho}}{\partial t} + \frac{\partial \langle \tilde{u}_i \rangle}{\partial x_i} = 0, \quad \frac{\partial \langle \tilde{u}_i \rangle}{\partial t} + \langle \tilde{u}_j \rangle \frac{\partial \langle \tilde{u}_i \rangle}{\partial x_j} = -\frac{1}{\rho}\frac{\partial \bar{p}}{\partial x_i} + \frac{\partial}{\partial x_j}\left[\nu \frac{\partial \langle \tilde{u}_i \rangle}{\partial x_j} - \langle u_i' u_j' \rangle\right] + (\bar{\rho} - \rho_\infty) g_i \quad (1)$$

The phase-averaged products of velocity fluctuations or Reynolds stresses in these equations are here obtained from the eddy-viscosity formula:

$$-<\overline{u_i'u_j'}>=<\nu_t>\left(\frac{\partial<\tilde{u}_i>}{\partial x_j}+\frac{\partial<\tilde{u}_j>}{\partial x_i}\right)-\frac{2}{3}\left[<\tilde{\nu}_t>\frac{\partial<\tilde{u}_i>}{\partial x_i}+<\tilde{k}>\right]\delta_{ij} \quad (2)$$

In the conventional k-ε model $<\tilde{\nu}_t>$ is related to the turbulence energy $<\tilde{k}>$ and its dissipation $<\varepsilon>$ as $<\tilde{\nu}_t>=C_\mu<\tilde{k}>^2/<\varepsilon>$ where $<\tilde{k}>$ and $<\varepsilon>$ are obtained from standard transport equations.

The standard k-ε model has been formulated and tested within steady-state calculation procedures against a range of plane shear flows with no distinct peaks in their energy spectrum. When a 2D time-dependent calculation is used part of the energy spectrum is directly resolved by this type of calculation. There is clearly ambiguity as to whether the standard model is capable of partitioning (correctly or at all) the total stress into its stochastic and periodic contributions (Koutmos and Mavridis, 1997).

In the present time-dependent calculations the spatial filtering due to the employed mesh is also accounted for in an effort to distinguish the directly computed (albeit 2D) turbulent motions, which are resolved by the mesh of size $\Delta(=(\Delta x \Delta y)^{1/2})$, from the turbulence already modelled and represented by the k-ε model. The eddy-viscosity is then evaluated by borrowing the Smagorinsky (1963) model from the LES formalism and the formulation representing the hybrid turbulence model (or mixed k-ε method) is as follows:

$$<\tilde{\nu}_t>=(C_s\Delta)^2(2<\tilde{S}_{ij}><\tilde{S}_{ij}>)^{1/2}$$

if

$$L_t=\frac{<\tilde{k}>^{3/2}}{<\tilde{\varepsilon}>}>\Delta$$

and

$$<\tilde{\nu}>=C_\mu\frac{<\tilde{k}>^2}{<\tilde{\varepsilon}>}$$

if

$$L_t<\Delta \quad (3)$$

C_S was here taken as 0.1. This choice was not found to be critical, however, since the above formulation takes into account the need for a variable C_S. The resulting ν_t is fed back into the production of k in the k-ε equations thereby producing a continuous distribution of ν_t and avoids inconsistencies in the boundaries between the regions where the two expressions of equation (3) are turned on. The internal iteration per time step, within the employed implicit scheme used here, is therefore well suited for this hybrid formulation. It should be noted here that as spatial resolution increases, i.e. the mesh is refined, the hybrid approach would not tend to an equivalent direct solution of the unaveraged equations as it would be expected of conventional 3D LES procedures. Within the present procedure

formal spatial averaging of the governing equations as in standard LES is not attempted; this here simply relies upon the mesh used and the k-ε eddy-viscosity is replaced from a mixing length model such as the Smagorinsky model when the length scale criterion is effective to reduce the error admitted by the standard k-ε. A conventional LES procedure of appropriate resolution therefore could perform as well as or even better than the present and more economic (due to its flexibility in grid node requirements) two-dimensional phase-averaged model. The above method also helped to obviate the need for a particular treatment of the k-ε model to avoid overshoots of k in the bar's forward stagnation point. Calculations with the standard k-ε model were clearly inferior to the hybrid method predictions both for the cold bluff-body flows, as has been demonstrated in Koutmos and Mavridis (1997), and for the present reacting bluff-body configurations as discussed in section 4 (see Figure 8) where conventional k-ε results are compared against hybrid computations.

3.2 Combustion model

In the thermochemical submodel a partial equilibrium scheme was used by constraining the gas state with respect to a pre-specified CO_2 concentration level. This corresponds to a two-scalar description employing the mixture fraction, f, and the CO_2 concentration, Y_{CO_2}. The reaction $CO+OH \leftrightarrow CO_2+H$, being one of the slowest (i.e. kinetically controlled) and most important in H/C oxidation, was employed to introduce the possibility of predicting non-equilibrium effects. CO_2 formation from CO is assumed to proceed primarily via this reaction and the overall reaction rate of CO_2 is obtained as:

$$\dot{r}_{CO_2} = k_f Y_{CO} Y_{OH} - \left(k_f / k_e\right) Y_{CO_2} Y_H \tag{4}$$

with k_f taken as $6.76^{*}10^{11}\exp(T/1102)$ and k_e obtained from the JANAF Thermochemical Tables (1971). Additionally, when the mixture strength exceeds the rich flammability limit the composition is taken as that of equilibrium at this limit diluted with pure fuel. Within this two-scalar description the final gas composition is calculated from the NASA equilibrium code (Gordon and McBride, 1976), for given f and Y_{CO_2} values by defining Y_{CO_2} as an "element". ρ, T, Y_i and $\dot{r}_{CO_2}$ values (the gas state vector) are then obtained in a 2D library for values $0<f<1$ and $0<Y_{CO_2}<Y_{CO_2,max}$. The evolution of the passive, f, and the reactive, Y_{CO_2} variables is calculated from the following equations:

$$\frac{\partial\left(\bar{\rho} < \tilde{f} >\right)}{\partial t} + \frac{\partial}{\partial x_j}\left(\bar{\rho} < \tilde{u}_j >< \tilde{f} >\right) = \frac{\partial}{\partial x_j}\left[\left(\bar{\rho}D + \frac{\mu_t}{Sc_t}\right)\frac{\partial < \tilde{f} >}{\partial x_j}\right] \tag{5}$$

$$\frac{\partial\left(\bar{\rho} < \tilde{Y}_{CO_2} >\right)}{\partial t} + \frac{\partial}{\partial x_j}\left(\bar{\rho} < \tilde{u}_j >< \tilde{Y}_{CO_2} >\right) = \frac{\partial}{\partial x_j}\left[\left(\bar{\rho}D + \frac{\mu_t}{Sc_t}\right)\frac{\partial < \tilde{Y}_{CO_2} >}{\partial x_j}\right] + \bar{\rho}\tilde{\dot{r}}_{CO_2} \tag{6}$$

with gradient transport assumptions for the turbulent fluxes $\widetilde{u'_j f'}$ and $\widetilde{u'_j Y'_{CO_2}}$.

An exponential joint PDF is constructed from the normalized mixture fraction and CO_2 concentration values, f^* and $Y^*_{CO_2}$, which are used to transform the physically allowable space of f and Y_{CO_2} into a normalized square area suitable for integration. The relationships established by this transformation are:

$$f^* = f + Y_{CO_2} / Y_{CO_2,air}, \quad Y^*_{CO_2} = Y_{CO_2} \Big/ \left(f \cdot Y_{CO_2,fuel} \right) \tag{7}$$

where:

$$Y_{CO_2,fuel} = nM_{CO_2} / M_{C_N H_M}, \quad Y_{CO_2,air} = M_{CO_2} \Big/ \left(M_{O_2} + M_{N_2} / 0.259 \right).$$

The local PDF is of the form:

$$P\left(f^*, Y^*_{CO_2} \right) = \exp\left[a_1 + a_2 f^* + a_3 Y^*_{CO_2} + a_4 f^{*2} + a_5 Y^{*2}_{CO_2} + a_6 f^* Y^*_{CO_2} \right] \tag{8}$$

This PDF shape was originally proposed by Pope (1979) as the most likely distribution for a turbulent scalar when the first and second moments are known. Furthermore, such a PDF shape is here considered as the most suitable for flame conditions close to extinction as inferred from the experimental data of Masri *et al.* (1988). The functional PDF form is calculated parametrically through the coefficients (a_1–a_6) which depend on the local moments $\widetilde{f'^2}$, $\widetilde{Y'^2_{CO_2}}$, $\widetilde{f'Y'_{CO_2}}$ which in turn are obtained assuming equilibrium between the turbulent production and destruction of these moments in their general form equation:

$$\frac{\partial\left(\bar{\rho}\widetilde{X'Z'}\right)}{\partial t} + \frac{\partial\left(\bar{\rho}\tilde{u}_j \widetilde{X'Z'}\right)}{\partial x_j} = \frac{\partial}{\partial x_j}\left[\left(\bar{\rho}D + \frac{\mu_t}{Sc_t}\right)\frac{\partial \widetilde{X'Z'}}{\partial x_j}\right] + 2\frac{\mu_t}{Sc_t}\left[\frac{\partial \tilde{X}}{\partial x_i}\frac{\partial \tilde{Z}}{\partial x_i}\right] - C_\Phi \bar{\rho}\frac{1}{\tau_t}\overline{X'Z'} + \overline{X'S_Z} + \overline{Z'S_X} \tag{9}$$

The moments are then obtained from the following expression:

$$\overline{X'Z'} = \frac{1}{2.0\bar{\rho}}\left[\frac{2\mu_t}{S_{Ct}}\frac{\partial \tilde{X}}{\partial x_i}\frac{\partial \tilde{Z}}{\partial x_i} + \overline{X'S_Z} + \overline{Z'S_X}\right]\tau_t \tag{10}$$

for $\tilde{X} = \langle \tilde{f} \rangle$ or $\langle \tilde{Y}_{CO_2} \rangle$ and $\tilde{Z} = \langle \tilde{f} \rangle$ or $\tilde{Y}_{CO_2} \rangle$, (C_ϕ = 2.0). Finally the PDF constants are determined from these moments from normalization conditions and expressions for the moments resulting from integration of the PDF form. Mean quantities such as density, temperature or source terms involving reaction rates and correlations are evaluated by using PDF information, e.g.

$$\tilde{\dot{r}}_{CO_2} = \frac{1}{\bar{\rho}} \int\int \dot{r}_{CO_2} J \rho \mathrm{P}\left(\mathrm{f}^*, \mathrm{Y}^*_{CO_2}\right) \mathrm{d}\mathrm{f}^* \mathrm{d}\mathrm{Y}^*_{CO_2} \tag{11}$$

where J is the Jacobian of the transformation of f, Y_{CO_2} and $\dot{r}_{CO_2}$ is the instantaneous reaction rate obtained from equation (4) as $\dot{r}_{CO_2} = \dot{r}_{CO_2}(f^*, Y^*_{CO_2})$. All the turbulent Prandtl/Schmidt numbers were taken equal to 0.6, a value which gave satisfactory results.

The eddy-viscosity appearing in the above expressions is obtained from equation (3). In line with the momentum field hybrid formulation the turbulent time scale, τ_t, appearing in equation (10) is evaluated as:

if

$$L_t > \Delta$$

then

$$\tau_t = \Delta / \sqrt{< \tilde{k} >}$$

and if

$$L_t < \Delta$$

then

$$\tau_t = < \tilde{k} > / < \tilde{\varepsilon} > \tag{12}$$

The buoyancy term $\bar{u}'' (\partial \bar{p}/\partial x_j)$ which appears in exact form in the <k> equation and in modelled form in the $<\varepsilon>$ equation is here modelled in the production of <k> as:

$$\frac{\mu_t}{\sigma} \frac{1}{\bar{\rho}} \frac{\partial p}{\partial x_i} \frac{\partial \bar{\rho}}{\partial x_i} + \frac{\rho_\infty}{\bar{\rho}^2} \frac{\mu_t}{\sigma} \frac{\partial \bar{\rho}}{\partial x_i} g_i \tag{13}$$

To account for finite-rate chemistry effects such as partial extinction and reignition the ratio of the local mixing time to the chemical time, i.e. the local Damkohler number, is monitored at each location in the reacting flow field. The inverse of the reaction rate supplied by the two-scalar partial equilibrium thermochemical model, $\dot{r}_{CO_2} = \dot{r}_{CO_2}(f^*, Y^*)$ is chosen here as the chemical time scale, τ_{ch}, as follows:

if

$$f_L < f < f_R$$

then

$$\tau_{ch} = \tau_{ch}\left(f^*, Y^*_{CO_2}\right)$$

if

$$f \le f_L$$

then

$$\tau_{ch} = \tau_{ch}\left(f_L^*, Y_{CO_2}^*\right)$$

if

$$f \ge f_R$$

then

$$\tau_{ch} = \tau_{ch}\left(f_R^*, Y_{CO_2}^*\right) \quad (14)$$

where $f_{L,R}$ are the lean and rich flammability limits respectively. In practice due to the asymptotic nature of τ_{ch} f_L and f_R, the time scale was evaluated at f_L+(10 percent) Δf_{RL} and f_R – (10 percent) Δf_{RL}, where $\Delta f_{RL}=f_R-f_L$. Figure 2a displays distributions of the instantaneous τ_{ch} from the present thermochemical model for methane and air at an inlet temperature and pressure of 300K and 1atm as a function of f and $Y^*_{CO_2}$. It is assumed that in the convective-diffusive lean or rich regions of the gas state, in f space, τ_{ch} is constant and equal to the value at the lean or rich limit respectively. The mean time-scale, τ_{ch}, obtained by integration along the lines of equation (11) is used in the extinction criterion described below. Extinction is predicted in a location whenever the following relationship holds true: $[\tau_t/\tau_{ch}]/[L_t/L_{R,t}]\le 1$. Then the chemical source terms appearing in equations (6) and (11) are set equal to zero whenever such conditions prevail. L_t and τ_t are the turbulent length and time scales evaluated through equations (3) and (12). $L_{R,t} = \sqrt{2}(\Delta f_{RL}/\Sigma_f)Re_t^{-3/4} * L_t$ is the reaction zone thickness in physical space as discussed in Masri *et al.* (1990). Re_t is the local turbulent Reynolds number and $\Delta f_{RL} = f_R - f_L$. For the lean and rich regions, i.e. when $f \le f_L$ or $f \ge f_R$ Δf_{RL} is replaced by f_L or $(1 - f_R)$ respectively. Σ_f in the above expression is the scalar or Gibson scale (Masri *et al.,* 1990) equal to $(\varepsilon_f * \tau_k)^{1/2}$ where ε_f is the dissipation rate of the scalar fluctuations and τ_k is the Kolmogorov time scale, $\tau_k = (\nu/\varepsilon)^{1/2}$. In effect the local chemical time-scale, τ_{ch}, is here compared with what is considered as the most relevant local mixing time affecting the reaction zone which is defined as: $\tau_m = L_{R,t}/\sqrt{2/3k} = \tau_t[\sqrt{2}\,(\Delta f/\Sigma_f)Re_t^{-3/4}]$. From this we may then obtain an expression for the quenching criterion containing only physically relevant quantities and no adjustable constants:

$$\frac{\tau_t}{\tau_{ch}} \le \frac{1}{\sqrt{2}} \frac{\Sigma_f}{\Delta f_{RL}} Re_t^{3/4} \quad (15)$$

Through this formulation the effect of the broadening of the reaction zone, e.g. due to dilution of fuel, in mixture fraction space, is accounted for to first order, and this is an aspect which has been particularly stressed in a number of works

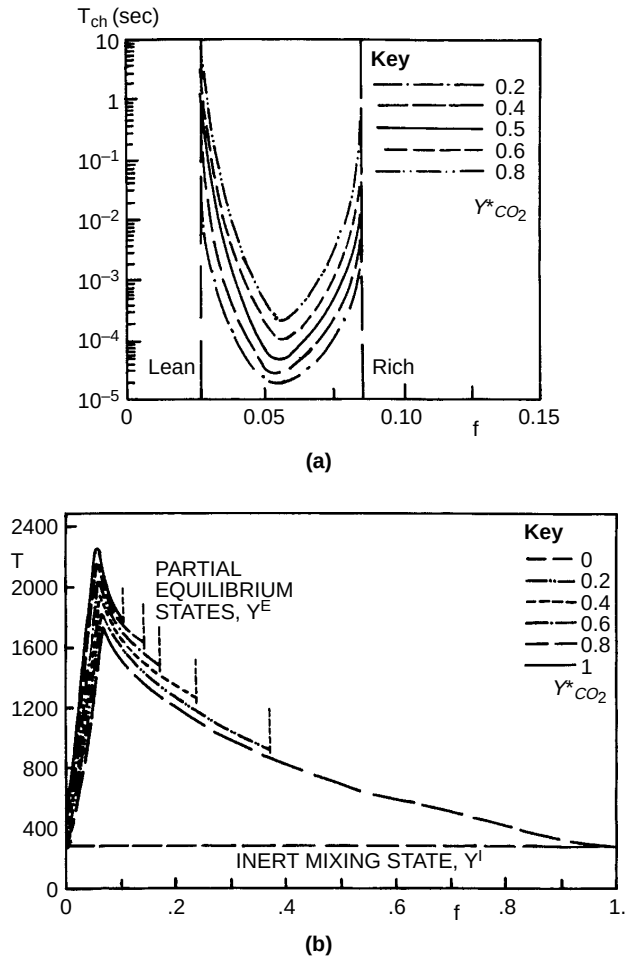

Figure 2.
(a) Partial equilibrium chemical time-scale plot for methane as a function of mixture fraction and normalised CO_2 mass fraction; (b) Reactive scalar profiles and considered gas states in a mixture fraction space

(Bilger, 1988; Masri *et al.,* 1990, 1994) in relation to the bimodal-monomodal flame behaviour as extinction is approached.

When extinction is detected the chemical source of the reactive scalar and the correlations involving the reaction rate are set to zero and the quenched region is treated as an inert mixing region. The gas state at any instant is therefore obtained either from the partial equilibrium state vector $Y^E = Y^E (f^*, Y^*_{CO_2})$, when the time scale criterion is inoperative, or from the non-reactive mixing between fuel and air state vector $Y^I = Y^I(f^*)$ when the criterion is valid (Figure 2b). Y represents the species considered, the temperature, the density or the instantaneous CO_2 reaction rate. In either case mean quantities at each time step are evaluated by integration (equation 11) using the PDF form. Such a treatment of the quenched region has been suggested in Peters (1988) and has been used in conjunction with a flamelet model. Reignition is allowed at any instant the strain is relieved, i.e. the criterion is invalid and the gas state is again

obtained from the partial equilibrium model. Clearly this limiting burning/non-burning approach ignores transient post-extinction non-reactive mixing or the possible reignition of the quenched mixture under partially premixed conditions; these are aspects that require further modeling, something which will be attempted in future work.

3.3 Numerical details

The low-Re model of Rodi *et al.* (1993) was adopted for the modelling of all wall regions. The simple convective boundary condition $\partial\phi/\partial t + U_0(\partial\phi/\partial x) = 0$, ($c = \bar{U}_0$), was used at the outlet and reduced the time required to achieve periodic conditions. Three meshes of 80×60, 120×85 and 175×123 (x,y) grid points were used with an axial expansion ratio of 1.1 for both bluff bodies. Predicted variables changed by 5.5 percent at the first level of grid refinement and by 1.5 percent at the second level. This refinement study suggested that the second mesh with clustering near the burner walls (the near wall node placed at $\Delta y/D = 10^{-3}$ i.e $y^+ = 0.1$ to 2) produced an acceptable level of fineness and accuracy for engineering purposes and was used for all presented results. For the square burner the inlet to the calculation domain was placed at 4.5 cylinder diameters upstream of the bluff-body while the inlet plane for the axisymmetric configuration was placed at the burner face. Inlet conditions were obtained in both cases from the experiments.

The solution of the set of the above equations was obtained with a finite-volume method based on a staggered mesh, a pressure correction method (SIMPLE) and the QUICK differencing scheme (Koutmos, 1985). A three-level-backward implicit Euler second-order scheme was used for temporal integration. Time steps were of the order $10^{-4} - 10^{-5}$s depending on Reynolds number and flame type (short or long) and run times on the HP 735 Risc System were about 12 hours. After an initial transient of about $30t_O$ ($t_O = D/U_O$) statistics were computed over approximately $100t_O$. The calculation of the total time-averaged RMS u and v values were here obtained with the help of the simple anisotropic model:

$$u_{i,RMS} = \left[u^2_{i,RMS,E} + \left(\frac{u^2_{i,RMS,E}}{0.5(1+\alpha)(U^2_{RMS,E} + V^2_{iMS,E})}\right)\bar{k}\right]^{1/2} \tag{16}$$

with i = 1,2. $u_{i,RMS,E}$ are the fluctuations resolved by the numerical procedure obtained explicitly (statistically) from the solution procedure (Koutmos and Mavridis, 1997). The time-averaged total fluctuation energy (modelled + resolved), $\bar{k}_t$, is equal to $\bar{k}_E + \bar{k}$, where k_E is the energy recovered by the time-dependent procedure, $\bar{k}_E = 1/2(U^2_{RMS,E} + V^2_{RMS,E})$ and $\bar{k}$ is the time-averaged value of <k> statistically obtained from the k-ε model. As the method is two-dimensional an assumption was introduced for the $w_{RMS,E}$ component, i.e. $W^2_{RMS,E} = \alpha(U^2 + V^2)_{RMS,E}$. According to literature surveys a tentative value of $\alpha = 0.2$ was chosen for the cylinder flows and 0.45 for the axisymmetric burner. In comparing density-weighted results with experiments it should be noted that

in general thin digitally-compensated thermocouples measure unweighted temperatures whereas the LDV measures density-weighted velocities (Libby and Williams, 1993; Masri *et al.,* 1988).

4. Results and discussion

The development of the two reacting flows is presented in the form of time-mean data and statistical quantities which are compared with the experimental data. The performance of the model is appraised and improvements suggested.

First the predictions for the long jet-like bluff-body flame are presented. In this case the fuel jet with high enough momentum penetrates through the primary (combustion products) recirculation induced by the bluff-body. Figure 3 displays the simulated overall reacting flow development in the form of time-averaged streaklines. With a fuel jet-to-annulus air velocity ratio (FAVR) of 3.47 this reacting flow operates in the jet-dominated regime (Correa and Gulati, 1992; Roquemore *et al.,* 1983; Schefer *et al.,* 1987) and recirculation effects are confined to the bluff-body base where flame stabilisation occurs. At this FAVR value the flame exhibits significant local extinction (Correa *et al.,* 1994) in the region of high mixing rates at about x/d = 20. It should be remarked that if the fuel velocity is further increased the rich blow-off limit of the flame will be reached. The present time-dependent predictions also confirmed the experimental finding that this flame type does not manifest any large scale periodic shedding.

Computed radial profiles of the mean and rms mixture fraction are compared in Figure 4a with experiments (Correa *et al.,* 1994). The good agreement shown lends strong support to the success of the present aerodynamic model and enables an appropriate evaluation of the combustion submodel. Figures 4b and 4c compare measured and predicted reactive scalars, mean temperature, methane and oxygen mass fractions at the regions of maximum turbulence where local extinction, i.e. finite-rate kinetic effects, are expected to be significant. The peak temperature is predicted well along the shear layer at $r \approx 0.01$, but it is under-estimated by more than 200K on the centre-line. The low peak temperature of only about 875-900K is evidently the result of partial extinction and its accurate reproduction lends support to the present combustion model. The model fails in the cooler fuel-rich region near the centre-line where both the partial equilibrium and the burning/non-burning mode assumptions may be questioned. Nonetheless, the present agreement is similar to that produced by a PDF transport method (Correa *et al.,* 1994).

Discrepancies between predictions and measurements increase in the comparisons of major species shown in Figure 4c. Although the partial equilibrium model by itself does not allow for any significant coexistence of fuel and oxygen the implementation of the present extinction model makes this possible. The calculated CH_4 and O_2 profiles follow closely the experimental trend despite the quantitative discrepancy. The overprediction of O_2 is consistent with the underprediction of temperature on the centre-line. The use of joint statistics between f and T is frequently used to study turbulence/chemistry interactions since they provide information on the mixing and the

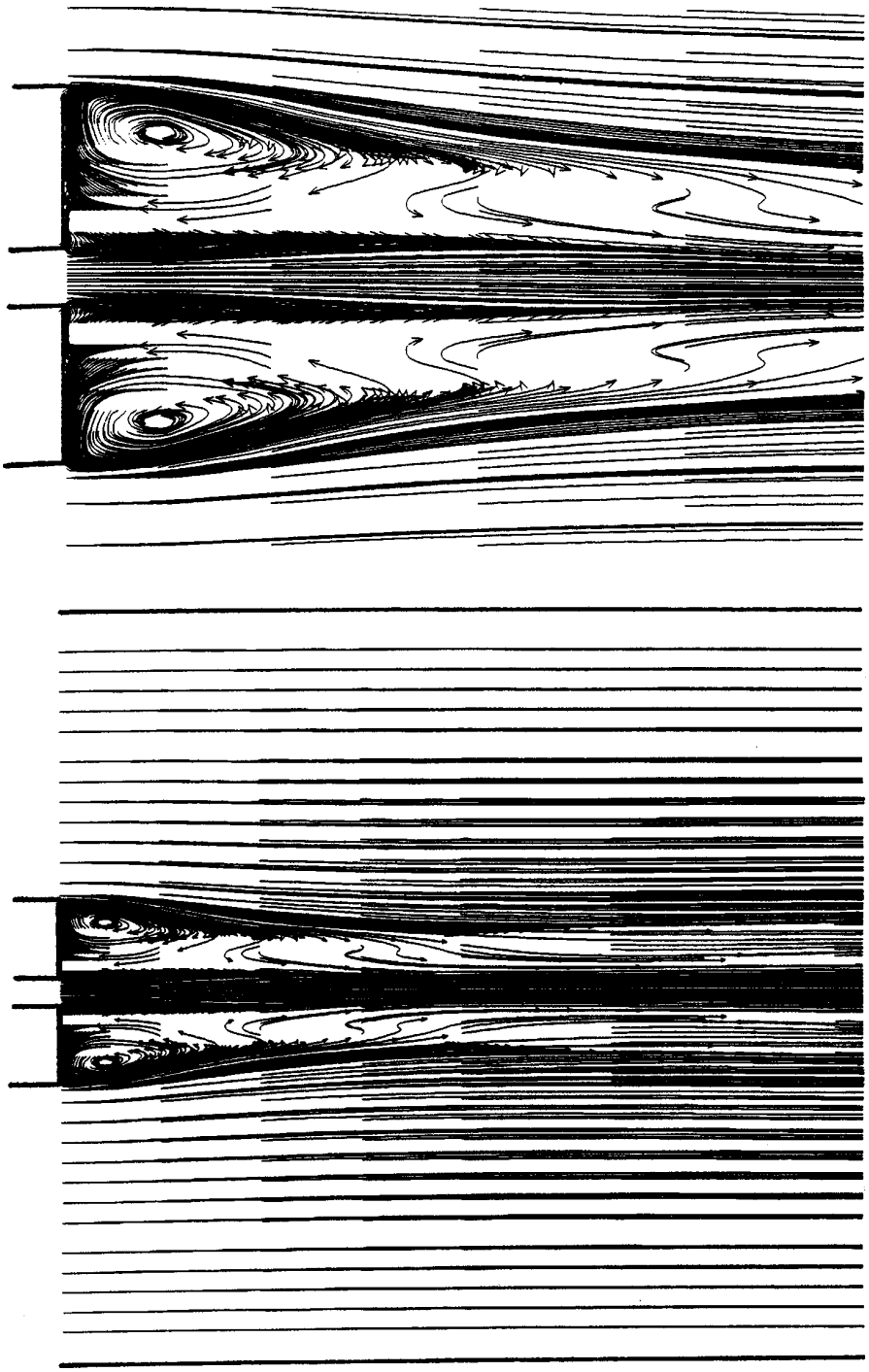

Figure 3.
Computed time-averaged streakline plot for axisymmetric burner

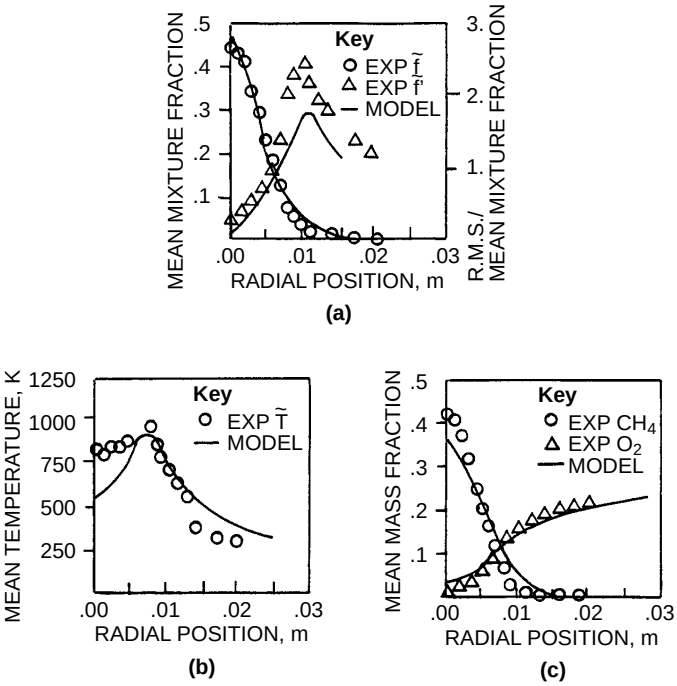

Figure 4. Comparisons of measured and calculated radial profiles of (a) mean and rms mixture faction; (b) mean temperature; (c) mean mass fractions of CH_4 and O_2 (x/d = 20)

reactedness of the gas state. The present time-dependent model produces such information and an f – T scatter plot is compared against the Raman data in Figure 5 for x/d = 20. Predicted points are located, some in the partial equilibrium region and most on the mixing line, as a result of the dual burning/non-burning mode operation of the present model, signifying the extent of local extinction at this position.

Although no periodic large scale motions were computed in the above flame the use of the time-dependent model is thought to be beneficial for a number of reasons:

(1) It outperforms steady-state standard k-ε procedures (Koutmos and Mavridis, 1997) and produces more accurate predictions of the turbulent mixing fields.

(2) The assumptions of the PDF shape in the combustion submodel may be less critical at the small (unresolved) scale level.

(3) The present time-scale extinction criterion and the two-mode burning/non-burning condition are more conveniently embodied within the time-dependent approach.

(4) The time-dependent procedure provides a more suitable vehicle for extending the model to handle transient post-extinction effects.

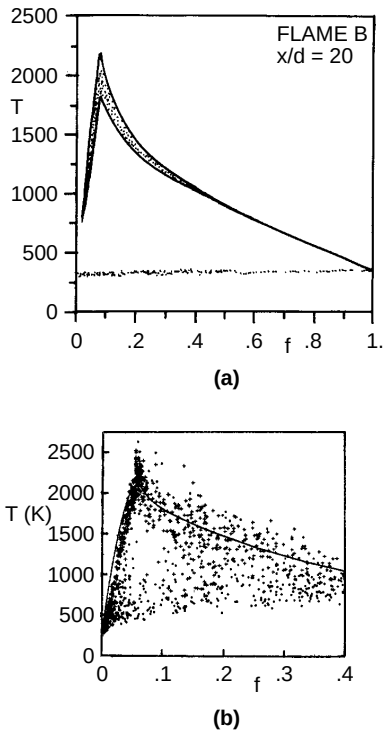

Figure 5.
Joint PDF scatter plot in the f-T space, x/d = 20, r/d = 0.5 ÷ 2.5, (a) computed; (b) experimental

The model's performance is examined next in the slender bluff-body flame configurations. At the lean FAVR range investigated, 0.631 to 0.110, the burner (Figure 1b) operates in the air-flow dominated regime with no fuel jet penetration through the primary recirculation. The overall reacting flow patterns for the three FAVR cases, 0.631, 0.189 and 0.155 are displayed in Figures 6a, 6b and 6c in the form of calculated time-averaged streakline plots. A system of four counter-rotating vortices was observed in both measurements and calculations within the recirculation region for the two higher FAVR cases (Figures 6a and 6b). The primary (products) vortex opposes the fuel jet which in part recirculates adjacent and upstream of the cylinder base and in part supplies the flanks of this vortex system where the flame sheets are stabilised. The model predicts an overall lean blow-off FAVR value of 0.140 while the experiments determined a value of 0.110. The streakline plot of Figure 6c, at a FAVR = 0.155, therefore represents an almost extinguished flame; the vortex width and length in this case are only marginally larger than those predicted in the uninjected isothermal wake shown in Figure 6d.

The present aerodynamic model has successfully predicted the periodic shedding dominating the uninjected cold wake (Koutmos and Mavridis, 1997). Under reacting conditions, far from the lean extinction limit, it has been shown (Koutmos *et al.,* 1996) that the shedding was severely suppressed and this was

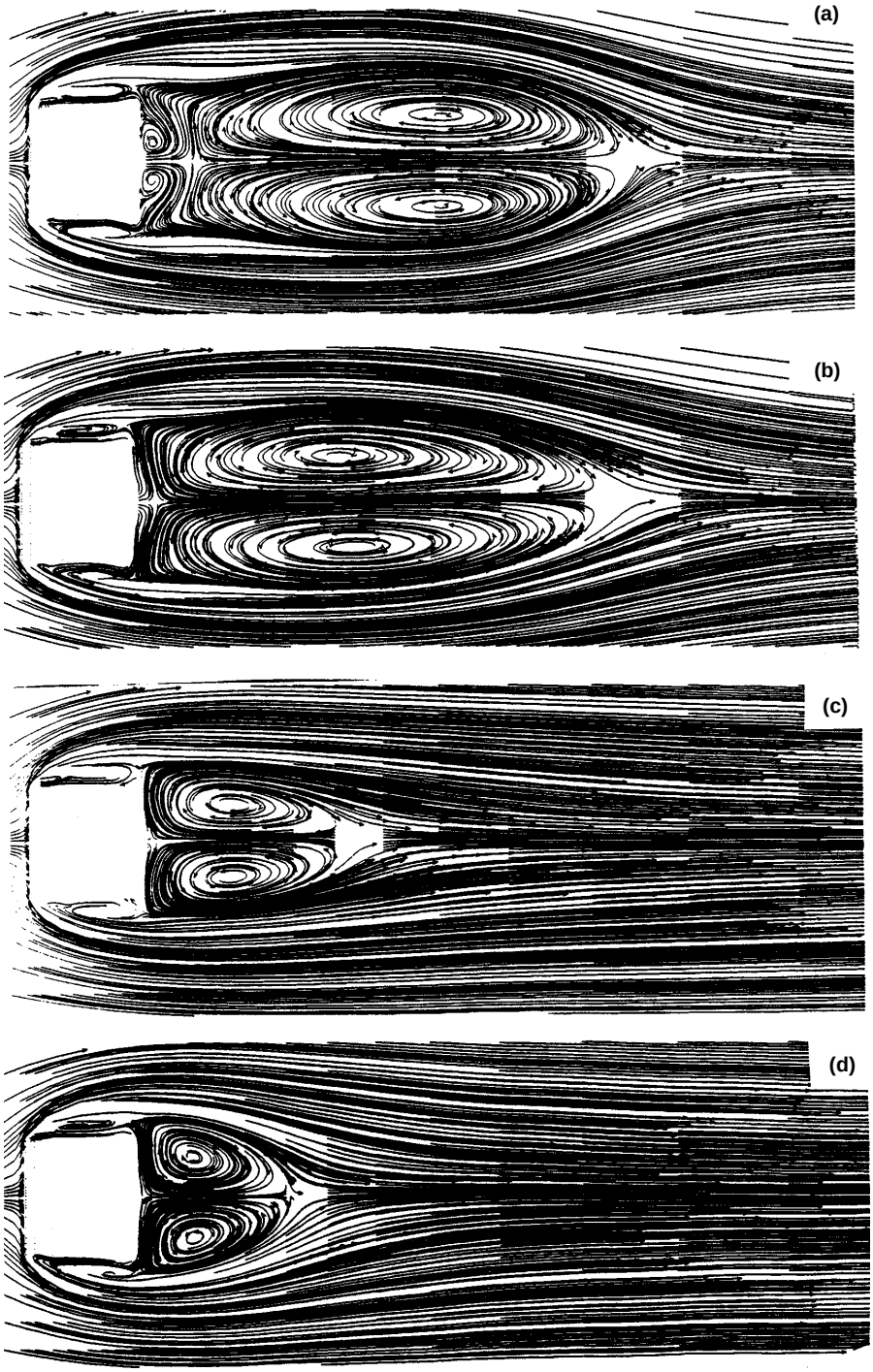

Figure 6. Computed time-averaged streakline plots for slender cylinder burner (a) FAVR = 0.631; (b) FAVR = 0.189; (c) FAVR = 0.155; (d) FAVR = 0.0 (isothermal)

attributed to laminarisation across the flame sheet (Figure 6a) which curtailed entrainment from outside the wake region. Here it is shown that near lean blow-off conditions, FAVR = 0.189, the periodic shedding reappears and becomes stronger as the lean extinction limit is approached. Figures 7a and 7b show measured and calculated V velocity spectra for the cases of FAVR 0.189 and 0.631 respectively. The broad frequency low energy peak evidenced in the high FAVR case (Figure 7b) becomes more distinct and approaches the basic Strouhal frequency of the isothermal cylinder wake at the low FAVR of 0.189 (Figure 7a), a trend well reproduced by the time-dependent procedure. The active role of large scale vortex structures is clearly enhanced as the flame gradually extinguishes in its downstream end while it shortens and stabilises on the two cylinder flanks attaining a two-tongued appearance.

The model's satisfactory performance can also be confirmed by the comparisons of measured and calculated axial distributions of mean velocity, turbulence kinetic energy and temperature along the symmetry plane illustrated in Figure 8a. In both experiment and computation vortex lengths under reacting conditions are about four times longer than the cold flow as a result of heat release and expansion. The effects of local extinction due to the intense mixing, as the flame shortens, in the vicinity of the primary recirculation stagnation position is clearly illustrated in the temperature profiles for the successive FAVRs of 0.631, 0.189 and 0.155 shown in Figure 8b. The combustion model seems to have faithfully reproduced the experimental trend with complete extinction of the flame predicted at a fuel jet velocity of 2.91 m/s compared to the experimental value of 2.3 m/s. Standard time-dependent k-ε computations are also included in Figure 8a. Evidently these significantly underpredict the recirculation length with attendant loss of the peak turbulence kinetic energy and temperature positions. It should also be remarked that as flame blow-off is approached and the quasi-periodic motion becomes more energetic the standard k-ε predictions worsen, a behaviour well expected (Koutmos and Mavridis, 1997).

The two bluff-body configurations studied span a wide range of operating conditions from the rich to the lean flame extinction limit. The present model

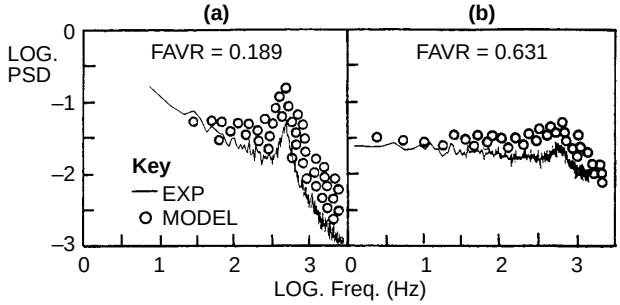

Figure 7.
(a) Measured and computed unormalized power spectra of the transverse (V) velocity for the square cylinder burner taken at (x/D, y/D) = (10.0, 0.0); (a) FAVR = 0.189; (b) FAVR = 0.631

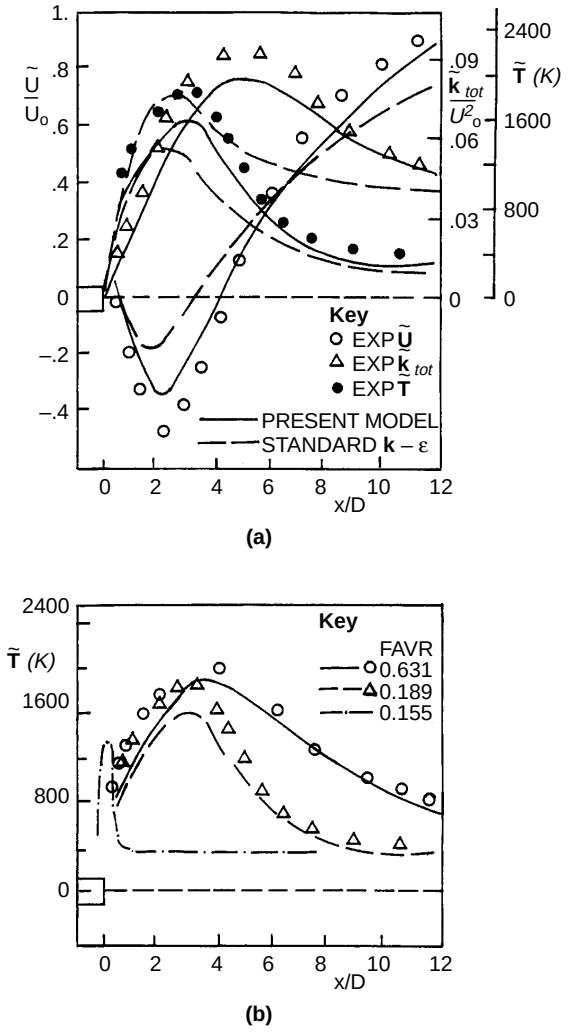

Figure 8. Measured and computed time-averaged distributions along the symmetry plane of (a) axial mean velocity, turbulence kinetic energy and mean temperature (FAVR = 0.189); (b) mean temperature for FAVR = 0.631, 0.189 and 0.155

has worked satisfactorily for both cases. Although the chemical time scale information was produced from a somewhat simplified chemistry the devised extinction criterion has proved effective. Possible areas of further improvement as regards the combustion model are the treatment of the post-extinction and reignition regimes. The post-extinction inert mixing of reactive scalars could be followed via a Lagrangian formulation for a mixing variable, something that might improve the discrepancies observed in Figures 4 and 8. The quenched mixture could possibly be considered that will reburn, under certain conditions, in a premixed fashion and treated by defining a further state vector, Y^P, obtained from premixed flame data.

5. Summary

A partial equilibrium/two-scalar exponential PDF turbulent combustion model was combined with a two-dimensional time-dependent hybrid Navier-Stokes procedure formulated by blending elements from both the LES methodology and the classical eddy-viscosity approaches. Local extinction effects were implemented by comparing the local rates of mixing and chemical reaction and appropriately setting the reaction rate of the reactive scalar to zero. The local gas state was obtained from a two-mode burning/non-burning combustion assumption. Detailed comparisons between measurements and calculations underlined the ability of the model to cope quite effectively with the range of complex reacting flows studied in the experiments under conditions of high or low-energy unsteadiness.

Despite its simplified chemistry and the neglect of the post-extinction and reignition regimes, the present approach adequately predicted significant effects of finite-rate kinetics under both lean and rich extinction conditions. With further tests and refinements the described method could be suitable for the study of combustor stability or reacting flows with active control of combustion.

References

Bakrozis, A., Papailiou, D. and Koutmos, P. (1994), "A study of slender bluff-body diffusion flame characteristics", University of Patras. Lab. Applied Thermod. MED, LAT-EXP-JOU1, January.

Bilger, R.W. (1988), "The structure of turbulent non-premixed flames", *22nd Int. Symposium on Combustion* (The Combustion Institute), pp. 475-88.

Cheng, T.S. and Pitz, R.W. (1994), "Simultaneous measurement of conserved and reactive scalars in turbulent diffusion flames for assessment of PDF models", *25th Int. Symposium on Combustion* (The Combustion Institute), pp. 1133-9.

Correa, S.M. and Gulati, A. (1992), "Measurements and modeling of a bluff-body stabilized flame", *Combustion and Flame*, Vol. 89, pp. 195-213.

Correa, S.M., Gulati, A. and Pope, S.B. (1994), "Raman measurements and joint PDF modeling of a non-premixed bluff-body stabilised methane flame", *25th Int. Symposium on Combustion* (The Combustion Institute), pp. 1167-73.

Gordon, S. and McBride, B.J. (1976), "Computer program for calculation of complex chemical equilibrium composition", NASA report SP-273.

Gran, I.R., Melaaen, M.C. and Magnussen, B.F. (1994), "Numerical simulation of local extinction effects in turbulent combustor flows of methane and air", *25th Int. Symposium on Combustion* (the Combustion Institute), pp. 1283-91.

JANAF Thermochemical Tables (1971), National Bureau of Standards Publications NSRDS-N3537.

Kaplan, C.R., Oran, E.S. and Back, S.W. (1994), "Stabilization mechanism of lifted jet diffusion flames", *25th Int. Symposium on Combustion* (The Combustion Institute), pp. 1183-9.

Koutmos P. (1985), "An isothermal study of gas turbine combustor flows", PhD Thesis, University of London.

Koutmos, P. and Mavridis, C. (1997), "A computational investigation of unsteady separated flows", *Int. Jnl. Heat and Fluid Flow,* Vol. 18 No. 2, pp. 297-306.

Koutmos, P., Mavridis, C. and Papailiou, D. (1996), "A study of turbulent diffusion flames formed by planar fuel injection into the wake formation region of a slender square cylinder", *26th Int. Symposium on Combustion* (The Combustion Institute).

Libby, P.A. and Williams, F.A. (1993), *Turbulent Reacting Flows*, Abacus Press, Tunbridge Wells.

Masri, A.R., Bilger, R.W. and Dibble, R.W. (1988), "Turbulent non-premixed flames of methane near extinction: mean structure from Raman measurements", *Combustion and Flame,* Vol. 71, pp. 245-66.

Masri, A.R., Bilger, R.W. and Dibble, R.W. (1990), "The local structure of turbulent non-premixed flames near extinction", *Combustion and Flame,* Vol. 81, pp. 260-76.

Masri, A.R., Dally, B.B., Barlow, R.S. and Carter, C.D. (1994), "The structure of the recirculation zone of a bluff-body combustor", *25th Int. Symposium on Combustion* (The Combustion Institute), pp. 1301-8.

Mellor, A.M. (1990), *Design of Modern Turbine Combustors*, Academic Press, New York, NY.

Neveu, F., Corbin, F., Trinite, M. and Perrin, M. (1996), "Simultaneous velocity and temperature measurements in a non-premixed bluff-body flame", *Ercoftac Bulletin*, No 26, September.

Obounou, M., Gonzalez, M. and Borghi, R. (1994), "A Lagrangian model for predicting turbulent diffusion flames with chemical kinetics effects", *25th Int. Symposium on Combustion* (The Combustion Institute), pp. 1107-13.

Ohiwa, N., Ishino, Y. and Yamaguchi, S. (1994), "Interactions between non-symmetrical wake structure and turbulent diffusion flames behind a rear-facing semicircular cylinder", *Combustion and Flame,* Vol. 99, pp. 302-10.

Peters, N. (1988), "Laminar flamelet concepts in turbulent combustion", *21st Int. Symposium on Combustion* (The Combustion Institute), pp. 1231-50.

Pope, S.B. (1979), "A rational method of determining probability distributions in turbulent reacting flows", *Jnl. Non-Equil. Thermod.*, Vol. 4, pp. 309-23.

Pope, S.B. (1990), "Computations of turbulent combustion: progress and challenges", *23rd Int. Symposium on Combustion* (The Combustion Institute), pp. 591-612.

Rodi, W., Mansour, N.N. and Michelassi, V. (1993), "One-equation near wall turbulence modeling with the aid of direct simulation data", *Jnl. Fluids Eng.,* Vol. 115, pp. 196-208.

Roquemore, W.M., Bradley, R.P., Stutrud, J.S., Reeves, C.M. and Obringer, C.A. (1983), *Utilization of Laser Diagnostics to Evaluate Combustor Models,* AGARD CP-353-36.

Schefer, R.W., Namazian, M. and Kelly, J. (1987), "Velocity measurements in a turbulent non-premixed bluff-body stabilised flames", *Combustion Science and Technology*, Vol. 56, pp. 101-38.

Smagorinsky, J. (1963), "General circulation experiments with the primitive equations", *Monthly Weather Review,* Vol. 91 No. 3, pp. 99-164.